Appl. Phys. B 84, 371–373 (2006)
DOI: 10.1007/s00340-006-2274-2

Applied Physics B
Lasers and Optics

A. FRIEDENAUER[1,✉,*]
F. MARKERT[1,*,**]
H. SCHMITZ[1]
L. PETERSEN[1]
S. KAHRA[1]
M. HERRMANN[1]
TH. UDEM[1,2]
T.W. HÄNSCH[1,2]
T. SCHÄTZ[1]

High power all solid state laser system near 280 nm

[1] Max-Planck-Institut für Quantenoptik, Hans-Kopfermann-Str. 1, 85748 Garching, Germany
[2] Ludwigs-Maximilians-Universität München, Schellingstr. 4, 80799 München, Germany

Received: 20 March 2006
Published online: 23 May 2006 • © Springer-Verlag 2006

ABSTRACT We present a stable high power all solid state laser system emitting 1-W of continuous wave laser radiation at a wavelength of 559 nm or 275 mW near 280 nm. The system consists of a commercial 2-W fiber laser with a line width of less than 200 kHz at 1118 nm and two home-built subsequent second harmonic generation external ring cavities using LBO and BBO crystals, respectively. The system is designed to act as a detection and cooling laser for trapped Mg^+ ions.

PACS 03.67.Lx; 32.80.Qk; 42.60.By; 42.79.Nv

1 Introduction

The fact that the laser apparatus for experiments with trapped light ions (Be^+, Mg^+) is very complex and expensive is one of the main obstacles for scaling up to larger multi-beam experiments. Due to the development of high power fiber laser systems with superb beam quality and low maintenance combined with efficient frequency quadruplers, this kind of experiment comes closer into consideration as these systems cost a fraction of the formerly used dye and related pump lasers. The laser source we present in this paper is actually used to detect and cool trapped Mg^+ ions driving the transitions from the ground state $3S_{1/2}$ to the $3P_{1/2}$ or $3P_{3/2}$ levels at approximately 280 nm.

2 Laser system

Acting as fundamental beam source, we use a commercially available 2-W ytterbium fiber laser at 1118 nm with a line width smaller than 200 kHz built by Koheras. The fiber laser consists of a fiber master oscillator and a power amplifier pigtailed by a non-polarization-maintaining fiber with an FC/APC connector. The laser is tunable both by temperature for slow tuning and by a piezo-controlled optical path length of the fiber allowing for a total scan range of 80 GHz with a bandwidth of 20 kHz at 1118 nm. We double the frequency of the laser output in the infrared (IR) twice by two subsequent second harmonic generation (SHG) cavities. We use 10 mW of the second-harmonic beam at 559 nm to implement polarization spectroscopy [1, 2] to stabilize the laser frequency to an appropriate iodine transition (R(53)28-3 at 559.271 nm) using the piezo of the laser. In addition to the power of 2 W at the wavelength of 1118 nm, the fiber laser emits 1.2 W of broadband amplified spontaneous emission (ASE) peaked between 1060 nm and 1100 nm. After switching on the power amplifier the laser undergoes polarization drifts which fall off exponentially in time. After about two hours the output polarization reaches a steady state provided that the non-polarization-maintaining fiber is fixed in position. We control the polarization of the beam coming from the single-mode fiber by quarter- and half-wave plates. We reduce the amount of retroreflected light into the laser by an optical isolator, which is designed for a wavelength of 1064 nm and transmits approximately 90% of the incident power at 1118 nm (isolation ≈ 30 dB) and half of the unpolarized ASE power, ending up with 1.8 W of pump power for the first SHG cavity. Since the ASE is not resonant with the cavity mode, it is filtered out by the optical resonator. We retrieve the incoupling efficiency by subtracting the ASE power from the total power. We mode match the pump beam into the first SHG cavity using two lenses, one of these being a fiber collimator with a variable distance between the end of the fiber and the lens.

3 SHG cavities

Frequency-doubling efficiencies up to 85% have been reported [3, 4] using type II phase matching in KTP crystals at wavelengths of 1060 or 1080 nm. Unfortunately, there is no possible non-critical type II phase match (NCPM) in KTP at 1118 nm [7]. Potentially usable crystals for doubling 1118 nm include potassium niobate (KNB, effective nonlinearity $d_{\text{eff}} = -12.1$ pm/V), lithium niobate (LNB, $d_{\text{eff}} = -4.4$ pm/V) or lithium triborate (LBO, $d_{\text{eff}} = 0.84$ pm/V). Although the niobate crystals have higher effective nonlinearities, the main advantage of LBO is its very high optical quality, high damage threshold and its moder-

✉ Fax: +49-89-32905-200, E-mail: axel.friedenauer@mpq.mpg.de
*Both A. Friedenauer and F. Markert contributed to this work equal parts.
**Present address*: Johannes-Gutenberg-Universität Mainz, Staudinger Weg 7, 55128 Mainz, Germany

ate NCPM temperature of 89 °C compared to 351 °C for KNB and 219 °C for MgO:LNB, which would be suitable for high-power applications.

For the first SHG cavity we use non-critically phase-matched, type I, α-cut lithium triborate (LBO) which is antireflective coated both for the fundamental and for the harmonic waves. The cutting angles of the crystal are $\theta = 90°$, $\varphi = 0°$; therefore, we obtain a round non-astigmatic green beam out of the cavity which can be coupled into the next cavity via two spherical lenses. The 18-mm-long crystal is placed inside an oven temperature controlled to within 20 mK. Theory predicts a phase-matching temperature of 89 °C, but we found optimum harmonic generation at 94 °C that might be due to improper heat contact between the copper oven and the crystal despite a thin indium foil in between. The crystal is placed in the smaller focus of a folded ring cavity (see Fig. 1). The cavity has a small folding angle of 10° (full angle between incident and reflected beams) at both focusing mirrors to minimize astigmatism. The total length of the ring cavity is 400 mm to ensure a large free spectral range (FSR = 750 MHz) and therefore a large resonance width of the longitudinal cavity modes.

As an input coupler we use a plane mirror with a reflectivity of $R = 97.5\%$ for the fundamental (M1, antireflective (AR) coated on the outside of the cavity) to impedance match the losses inside the cavity. The second mirror, highly reflective (M2, $R > 99.98\%$), is mounted on a small stacked piezo with high resonance frequency (Thorlabs model AE020304D04, $\nu_{\mathrm{res}} \approx 18$ kHz loaded). We glued the piezo to a disk made of lead to absorb vibrations and reduce the resonance frequency of the mirror mount. The dimension of this mirror is very small, allowing for a high servo bandwidth ($3 \times 3 \times 2\,\mathrm{mm}^3$). Furthermore, two curved mirrors of focal length $f = 25$ mm are used, one of them highly reflective at the fundamental (M3, $R > 99.98\%$), the other acting as an output coupler highly reflective at the fundamental (M4, $R > 99.9\%$) and highly transmissive at the harmonic wavelength ($T > 95\%$). The output coupler is shaped as a 'zero lens' and AR coated for the harmonic on the convex side. We modeled the cavity including linear and conversion losses of the crystal and reflection losses of the mirrors to determine the optimum crystal length of 18 mm. We derived the optimum focus inside the crystal from calculations following Boyd–Kleinman theory [5] to be 27.3-μm beam waist ($1/e^2$ of the intensity) and adjusted the distance between the curved mirrors to match this value at the plateau of the stability region (geometric distance between focusing mirrors M3 and M4: $d = 62$ mm). For stabilizing the length of the cavity we use the polarization-locking scheme of [6]. We obtain 1 W of green output power at 559 nm. For long-term operation, one can increase the stability of the system by further tilting the input polarization with respect to the crystal axis, sacrificing some output power for a stronger error signal. In this way we obtain a stable output power of 950 mW, corresponding to a conversion efficiency of the LBO resonator of larger than 52.7%. We stress that we give the available output power relative to the laser power in front of the cavity rather than correcting for coupling efficiency, Fresnel losses and output coupler loss.

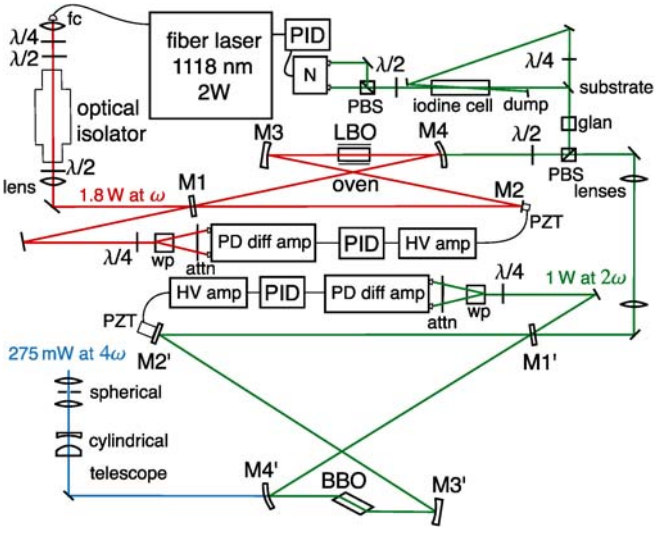

FIGURE 1 Optical setup of the laser system. The light coming from the fiber laser is collimated by the fiber collimator (fc) and passes the optical isolator after polarization adjustment by quarter- and half-wave plates ($\lambda/4$ and $\lambda/2$). After passing another half-wave plate the beam is mode matched (lens) into the LBO cavity consisting of mirrors M1, M2, M3 and M4. The light reflected at M1 passes a quarter-wave plate and a Wollaston prism (wp), is attenuated (attn) and falls on a photodiode (PD) differential amplifier. That signal goes to a proportional-integral-derivative (PID) servo and after amplification (HV amp) is fed to the piezo (PZT) on which the mirror M2 is mounted. The second-harmonic beam generated in the LBO crystal leaves the cavity via the output coupler M4 and 10 mW are separated from the beam for the iodine lock using a half-wave plate and a polarizing beam splitter (PBS). With this beam we implement polarization spectroscopy [2] using a Glan laser polarizer (glan) and a New Focus Nirvana photodetector (N). The larger part traversing the PBS is mode matched in the BBO cavity consisting of mirrors M1', M2', M3' and M4' using two mode-matching lenses. The generation of the error signal is identical to the first cavity. The ultraviolet beam generated in the BBO crystal leaves the cavity via M4' and is projected into a Gaussian TEM00 mode and collimated with the help of cylindrical and spherical telescopes. The whole setup fits on a breadboard measuring $90 \times 30\,\mathrm{cm}^2$ and is moveable

The output of the first cavity is coupled into an astigmatism-compensated second cavity based on a Brewster-cut BBO crystal, which we heat to approximately 50 °C in order to prevent water from condensing on the hygroscopic, polished surfaces of the crystal. The BBO crystal ($4 \times 4 \times 10\,\mathrm{mm}^3$) is mounted on a rotational and a linear translation stage which preserves distances and angles between the crystal and the focusing mirrors. Again, calculations following Boyd–Kleinman theory are carried out leading to an ideal focus of 19.4 μm. Mode matching the incoupling beam to the mode of the second SHG cavity is performed by two lenses mounted on 3D translational stages to ease realigning. The layout of the second cavity is similar to the first, differing only in the reflectivities of the mirrors and the folding angle of the cavity at both mirrors (full angle 27.4°) to compensate for the astigmatism caused by the Brewster-cut BBO crystal. We implemented this cavity using mirrors (M2', M3') with $R > 99.93\%$ and the

	LBO cavity	BBO cavity
Highly reflective (HR) mirrors fundamental	99.98%	99.93%
Output coupler HR fund.	99.9%	99.8%
Input coupler fund.	97.5%	98.4%
Distance between focusing mirrors	62 mm	59.4 mm
Total cavity length	400 mm	470 mm
Full folding angle	10°	27.4°
Incoupling power	1.80 W	0.95 W
Output power	0.95 W	0.275 W
Doubling efficiency	52.7%	28.9%

TABLE 1 Mirror reflectivities, measures and technical data of the SHG cavities

output coupler (M4') $R > 99.8\%$ at 560 nm and $T > 94\%$ at 280 nm. We project 95% of the astigmatic beam exiting the second cavity into a Gaussian TEM00 mode using a cylindrical telescope and collimate the beam using a spherical cleaning telescope. We end up with 275 mW of ultraviolet output power. Measures, mirror reflectivities and efficiencies of both cavities are summarized in Table 1.

4 Resonances

We discovered a 14-GHz-broad frequency region between 1118.409 nm and 1118.339 nm where we observe the following: when scanning the cavity length in one direction the transmission fringes are broadened while by scanning it backwards the fringes are narrowed. We were not able to lock the cavity in this frequency domain. We reproduced this phenomenon using several lasers, cavities and crystals. We note that all crystals were bought from the same crystal manufacturer (Crystals of Siberia). This frequency domain (quadrupled to the ultraviolet) does not overlap with the resonant transitions of Mg^+ isotopes from the ground state $3S_{1/2}$ to the $3P_{1/2}$ or $3P_{3/2}$ levels. But, it imposes restrictions for two-photon stimulated Raman transitions via detuned levels. It seems as if the index of refraction of the crystal changes with light intensity in the crystal. Previously, resonances of OH groups in LBO crystals have been found [8] with a comparable width however at different wavelengths than observed here.

5 Stability

We observe fluctuations in the ultraviolet (UV) output power within 2% deviation from the mean value. Furthermore, on microsecond time scales we notice regular drops of the UV output power smaller than 4%. Drops larger than 7% appear less than once a minute. In addition, we discover a sensitivity to long-term temperature drifts of the environment which resulted in oscillations as large as 10% of the output power as the temperature changed by 2 K, but we were able to reduce these drifts to 5% by proper thermal isolation of the crystal oven. The other problem is that the output polarization of the laser changes as the heat sink of the power amplifier of the fiber laser changes in temperature. Thus, the beam which is no longer parallel polarized with respect to the input polarizer of the optical isolator is not completely transmitted through the optical isolator. One has to manually adjust the output polarization of the fiber with the help of the quarter- and the half-wave plates to retrieve optimum transmission through the optical isolator. One solution to this issue could be an active stabilization of the temperature of the heat sink of the laser with the help of a Peltier element.

6 Conclusion

In summary, we presented a laser system consisting of a commercial ytterbium fiber laser and two subsequent external second harmonic generation ring cavities with an output power of 275 mW near 280 nm. This corresponds to an overall conversion efficiency of 15.2%.

ACKNOWLEDGEMENTS We thank Ove Poulsen, Jim Bergquist and Dietrich Leibfried for their genuine input and triggering ideas. We gratefully acknowledge financial support by the Deutsche Forschungsgemeinschaft and the Max-Planck-Institut für Quantenoptik.

REFERENCES

1 C. Wieman, T.W. Hänsch, Phys. Rev. Lett. **36**, 1170 (1976)
2 C.P. Pearman, C.S. Adams, S.G. Cox, P.F. Griffin, D.A. Smith, I.G. Hughes, J. Phys. B **35**, 5141 (2002)
3 R. Paschotta, K. Fiedler, P. Kürz, R. Henking, S. Schiller, J. Mlynek, Opt. Lett. **19**, 1325 (1994)
4 Z.Y. Ou, S.F. Pereira, E.S. Polzik, H.J. Kimble, Opt. Lett. **17**, 640 (1992)
5 G.D. Boyd, D.A. Kleinman, J. Appl. Phys. **39**, 3597 (1968)
6 T.W. Hänsch, B. Couillaud, Opt. Commun. **35**, 441 (1980)
7 All crystal data taken from SNLO program by Sandia National Laboratories
8 L. Kovács, K. Polgár, A. Péter, R. Capelletti, Mikrochim. Acta Suppl. **14**, 523 (1997)